

Millimeter-wave Beam-Scanning Antennas using Liquid Crystals

Gerardo Perez-Palomino , José. A. Encinar , Mariano Barba , Robert Cahill , Raymond Dickie , Paul Baine , and Michael Bain

Abstract— Two Liquid crystal-based reflectarrays that operate at 100 GHz and 125 GHz are presented. The first prototype (100 GHz) is used to validate the modeling and the design procedure proposed for this class of antenna. Experimental validation of the beam scanning is carried out by measuring the received power in a quasi-optical test bench, which is able to rotate the receiver in the horizontal plane. These results are used to design a second prototype antenna (125 GHz) which exhibits 2D beam scanning capabilities with a large bandwidth and scanning range that is sufficient for radar and communications applications.

I. INTRODUCTION

Liquid crystals (LC) offer an attractive alternative to conventional phase shifter technologies for creating high gain beam scanning antennas. The permittivity of the material can be changed by applying a quasi-DC signal, and the observed tunability is obtained over a large range of frequencies (from MHz to THz).

In the case of phased array antennas, a demonstrator based on this technology has been recently reported in [1], and the results obtained show that LC is an attractive alternative or complement to other phase shifter technologies at microwave frequencies. At higher frequencies (above 60 GHz), the manufacturing complexity is significantly increased, mainly because of the requirement to integrate the LC phase-shifters with both the RF feeding network and the biasing lines. To eliminate the complexity and losses produced by the beam-forming network, an external RF feed source, such as in the case of a reflectarray, is preferred. Taking into account that cells composed of printed resonant elements placed above a LC substrate offer a high degree of flexibility to tune the reflection phase in a simple array configuration, planar reflectarrays are able to take full advantage of the LC properties to produce low-cost beam scanning antennas operating in millimetre to sub-millimetre wavelengths [2]-[3].

II. LC-BASED REFLECTARRAY CELLS

A. Design Procedure

A LC-based reconfigurable reflectarray is shown in Fig. 1. The antenna is composed of two wafers of rigid material, which are separated by spacers to create a cavity that is filled with LC. The lower face of the top wafer (see Fig. 1) is printed with the resonant elements (patches, dipoles, etc) and

the upper face of the bottom wafer is clad with metal to form a conductive ground plane. Each of the reflectarray cells is biased by a quasi-DC voltage so that the permittivity (and phase-shift) necessary to obtain the desired radiation pattern is obtained spatially across the antenna aperture.

In this work, two LC-based reflectarray antennas are presented, which operate at 100 GHz and 125 GHz and use the LC mixture GT3-23001 which is manufactured by Merck KGaA. Two quartz wafers of 550 μm thick are used as superstrate and substrate of both designs. The characteristic parameters of the LC mixture have been provided by Merck at 19 GHz: $\epsilon_{r//} = 3.3$, $\tan\delta_{//} = 0.0038$, $\epsilon_{r\perp} = 2.5$, $\tan\delta_{\perp} = 0.0143$, and have been measured in the band from 140 to 165 GHz using a FSS [4]: $\epsilon_{r//} = 3.25$, $\tan\delta_{//} = 0.015$, $\epsilon_{r\perp} = 2.47$, $\tan\delta_{\perp} = 0.02$. The latter values have been used to design the reflectarray cells.

The unit cells employ three unequal length dipoles printed on the same plane [5]. The two prototypes are designed by using the two extreme states of permittivity, which are defined from the corresponding permittivity tensor. An isotropic effective permittivity that is extracted from each tensor is used to improve the computational efficiency. The design must provide more than 320° of phase range in a relatively large bandwidth and low sensitivity to the transversal inhomogeneity of the LC. More details about the design procedure can be found in [5].

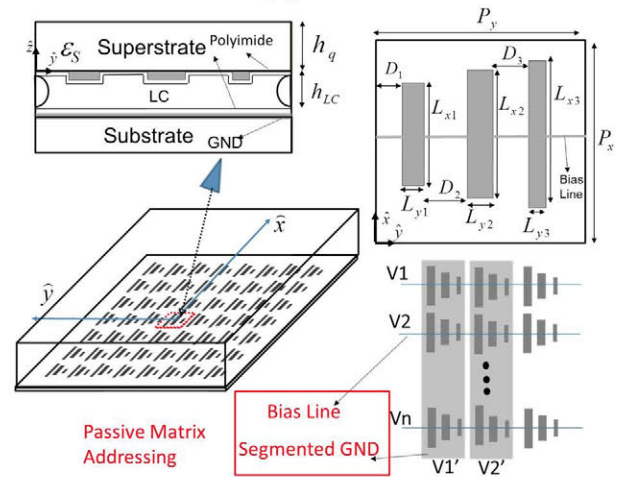


Fig. 1 LC-based Reflectarray. Structure for passive voltage addressing.

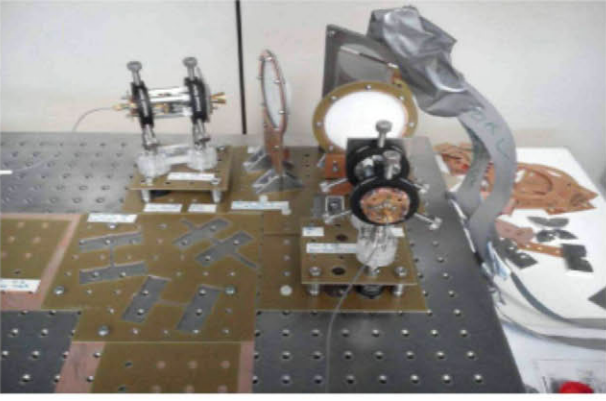
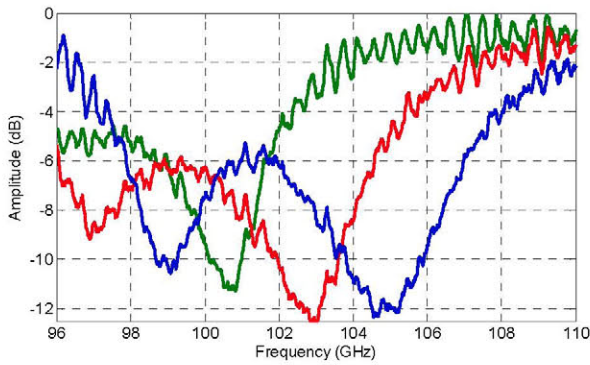
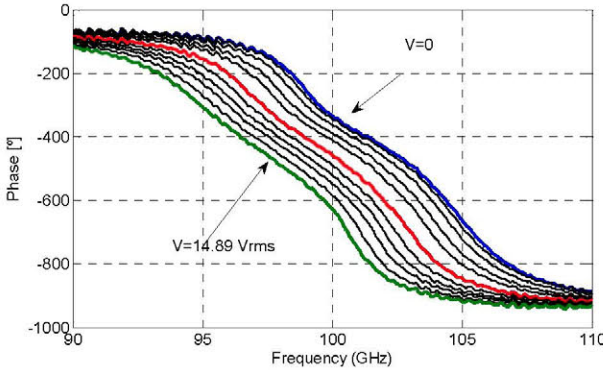


Fig. 2 LC-based reflectarray placed in the quasi-optical test bench in 30°/45° configuration (30° incidence, 45° reflection) used to characterize the LC-based antenna.



(a)



(b)

Fig. 3 Measured reflection amplitude and phase of the reflectarray designed at 100 GHz with all the cells identically biased, for several voltages and frequencies (three voltages for the amplitude). Angle of incidence, $\theta=30^\circ$, $\phi=0^\circ$, (30°/30° configuration). Waveform for AC biasing: 20 KHz -sine

B. Fabrication

The first prototype (100 GHz) has been constructed and tested to validate the modeling and the design process used for this type of antenna. The dimensions for the cells that form the antenna (54x52 elements) are reported in [5].

Three steps are required to complete the construction of the prototype: a) manufacture of the ground plane, b) deposition of a thin rubbed polyimide layer at each surface that forms the gap to anchor the liquid crystal molecules, and c) placement of precision shims to create the required wafer separation, and the subsequent bonding of the two wafers to form the gap which is filled with liquid crystals.

The ground plane has two functions: 1) to provide a conductive backing for the reflectarray thus permitting the creation of resonant elements in RF that achieve the required phase-shift, and 2) to permit the application of a control voltage across the cavity containing the liquid crystals, thus creating an electrostatic field that is used to rotate the molecules and to change the permittivity tensor.

In our case, the bias voltage is applied by using a passive LC matrix (see Fig. 1), which can be used for 2D voltage addressing. The ground plane is segmented into strips each of which cover a certain column of cells, whereas that the elements that form each row of elements are interconnected by a bias line [6]. The ground plane and the resonant elements (together with the bias lines) are printed on each surface by using photolithography, which ensures accuracy of around $\pm 2 \mu\text{m}$ for the metallization sizes.

In order to effectively align the LC director parallel to the cell substrate at repose, an appropriate surface treatment is required on the inside of the two cell surfaces. This is achieved using a rubbed polyimide thin film. The alignment layer is formed in two stages. Firstly a thin ($0.9 \mu\text{m}$) film of polyimide was deposited onto one side of the two cell substrates by spin coating the polyimide solution onto the patterned side of the quartz and metallised silicon surfaces at 5000 rpm for 1 minute. In the second stage the polyimide film was unidirectionally rubbed using a custom built rubbing machine.

The spacers are fabricated using small pieces of optical fiber whose cover was removed, which are dipped in epoxy resin and spaced apart on the quartz substrate. This technique ensures an accuracy of around $\pm 7 \mu\text{m}$ for the cell thickness.

Once the cavity is fabricated, a vacuum filling technique was used to insert the liquid crystals in the cavity. The empty liquid crystal cell must be placed in a vacuum chamber mounted above the crucible containing the liquid crystal fluid. Due to the capillary flow principle, liquid crystal starts to flow into the cell through the inlet port.

C. Experimental validation

To validate the first prototype (100 GHz) in a periodic environment ($\theta=30^\circ$, $\phi=0^\circ$), a quasi-optical test bench (see Fig. 2) has been used. Transmitter and receiver horns were symmetrically located respect to the reflectarray surface in the incident and reflected directions. Fig. 3 shows the measured amplitude and phase curves at several voltages in the band from 90 GHz to 110 GHz, for which the entire array is biased with the same voltage. The electrical performance of the cells is reported in Table I.

A. Test in quasi-Optical Bench

The reflection phase versus voltage plots are used to find the appropriate voltage distribution to scan the beam in the quasi-optical test bench and hence demonstrate electronic beam scanning of the whole reflectarray antenna. Fig. 4 shows the measured power when the signal is incident on the reflectarray at 30° and the receiver horn is located at 45° . In this case, the LC is biased to deflect the beam $+0^\circ$ (blue curve), -7.5° (red curve) and -15° (green curve) with respect to the specular direction (30°). It can be observed from Fig. 4 that by applying an appropriate voltage, the beam is scanned in the desired direction (45°), and the power is nearly constant in the band from 95 GHz to 105 GHz, which suggests that a large bandwidth is obtained. Fig. 5 shows the beam scanning capabilities as demonstrated above, but assuming a measured power when the signal is incident on the reflectarray at 30° and the receiver horn is located at 37.5° .

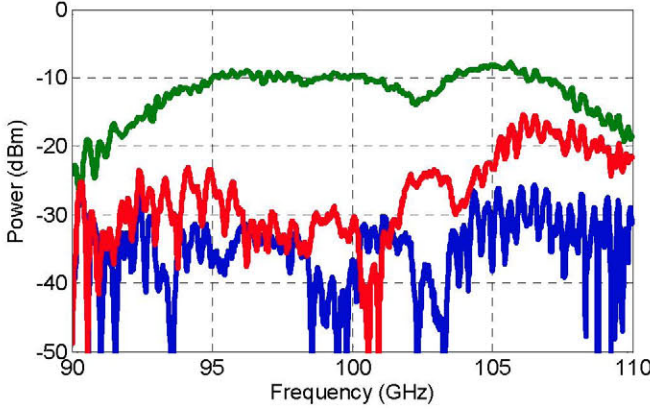


Fig. 4 Measured power when the LC is applied by a voltage distribution that deflects the beam $+0^\circ$ (blue), -7.5° (red) and -15° (green) in elevation. Configuration: $30^\circ/45^\circ$.

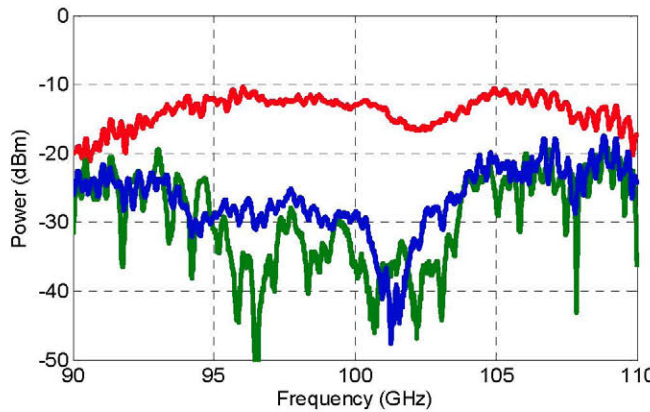


Fig. 5 Measured power when the LC is applied by a voltage distribution that deflects the beam $+0^\circ$ (blue), -7.5° (red) and -15° (green) in elevation. Configuration: $30^\circ/37.5^\circ$.

B. Design of Reflectarray at 125 GHz

A second prototype composed of 60×60 unit cells was designed to obtain a beam that can be scanned and collimated at 125 GHz. The horn is located in the coordinates $(-34, 0, 90)$ mm (see Fig. 1), and the cell dimensions are: $P_x=1.05$, $P_y=0.9$, $L_y1=0.52$, $L_y2=0.555$, $L_y3=0.6$, $L_x1=0.12$, $L_x2=0.15$, $L_x3=0.15$, $D1=0.115$, $D2=0.215$, $D3=0.15$, $h_{lc}=0.125$, $h_s=0.55$ (mm). The simulated amplitude and phase of the extreme states of permittivity are shown in Fig. 6 for several angles of incidence, and the electrical performance of the cells is also reported in Table I.

Fig. 7 shows the simulated radiation patterns (elevation and azimuth) at the scanning angle (20° from the boresight direction) at the centre (125 GHz) and two edges of band frequencies (120/130 GHz). The radiation patterns by using ideal phase-shifters are also plotted.

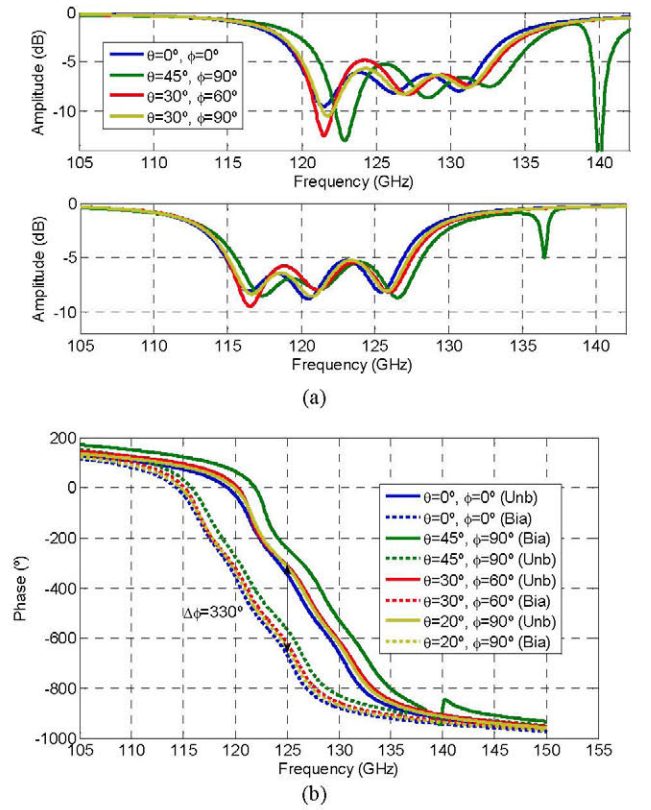


Fig. 6 Simulated (a) amplitude and (b) phase of the reflection coefficient as a function of frequency for different angles of incidence and the two extremes states of permittivity for the prototype 2.

TABLE I

Design	Bandwidth (%)	Losses (dB)	Phase Range ($^\circ$)	Sensitivity AOI ($^\circ$)
Prototype 1 (100 GHz)	8	8	320 ± 35	20
Prototype 1 (125 GHz)	8	6.5	330 ± 15	15

AOI: Angle of incidence.

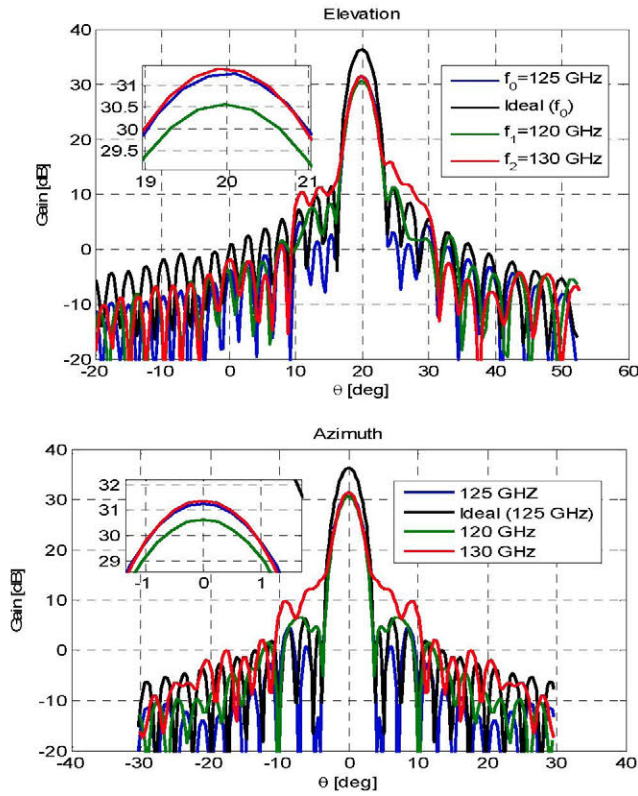


Fig. 7 Simulated radiation patterns (elevation and azimuth planes) of the prototype designed at 125 GHz for the beam scanned and collimated in the direction, $\theta = 20^\circ$, $\phi = 0^\circ$. Frequencies: 120, 125 and 130 GHz.

The simulations of the radiation patterns are obtained by considering the isotropic effective permittivity of the LC, whose range of variation was extracted from the tensors in extreme biasing states [5]. As can be noted, a reduction in the antenna gain from 36.35 dB to 30.21 (6.14 dB) is produced at the central frequency. These results are consistent with the average losses of the unit-cell, which are around 6.5 dB. Thus, the reduction in the antenna gain is produced mainly by the losses in the unit-cells. The lateral lobe levels remain similar or better than the ideal case in both, the elevation and azimuth planes, at central frequency. At the extreme frequencies, the gain is reduced 0.15 dB when compared with the gain at central frequency, and the side lobes are increased.

The simulated radiation patterns in elevation and azimuth for two scanning angles, $(\theta = 10^\circ, \phi = 0)$ and $(\theta = 30^\circ, \phi = 0)$ are also shown at different frequencies in Fig.8. In both cases, the radiation patterns exhibit similar gain and frequency behavior than in the case of the beam pointing to $\theta = 20^\circ$, with practically no beam squint (less than 0.3° at 130 GHz).

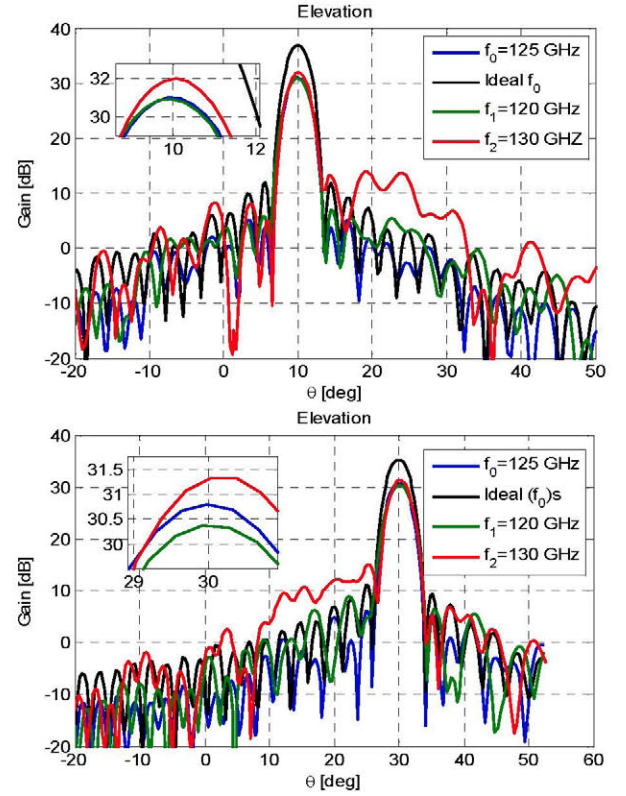


Fig. 8 Simulated radiation patterns (elevation plane) of the prototype designed at 125 GHz for the beam scanned and collimated in the directions, $\theta = 10^\circ$, $\phi = 0^\circ$ and $\theta = 30^\circ$, $\phi = 0^\circ$. Frequencies: 120, 125 and 130 GHz.

The results presented in this section demonstrate that the reflectarray can be used to provide electronically beam scanning in a frequency band better than 8%, with small distortions in the radiation patterns, practically no gain variations and no beam squint. The most severe limitation of these results is that the ohmic losses (mostly from the LC) produce a reduction in gain. This number can be reduced by improving the properties of the LC and/or by a multi-layer LC reflectarray cell.

REFERENCES

- [1] O. H. Karabey, et al., "A 2-D Electronically Steered Phased-Array Antenna With 2x2 Elements in LC Display Technology," *IEEE Trans. Microw Theory Tech.*, vol. 60, no. 5, pp. 1297-1306, May. 2012.
- [2] W. Hu, et al., "Liquid-crystal-based reflectarray antenna with electronically switchable monopulse patterns," *Electron. Lett.*, vol. 43, no. 14, pp. 744-745, 2007.
- [3] A. Moessinger, et al., "Electronically reconfigurable reflectarray with nematic liquid crystal," *Electron. Lett.*, vol. 42, no. 16, pp. 899-900, Aug. 2006.
- [4] R. Dickie, et al., "Electrical characterisation of liquid crystals at millimetre wavelengths using frequency selective surfaces" *Electron Lett.*, vol. 48, no. 11, pp. 611-612, May. 2012.
- [5] G. Perez-Palomino, et al., "Design and Experimental Validation of Liquid Crystal-Based Reconfigurable Reflectarray Elements With Improved Bandwidth in F-Band," *IEEE Trans. Antennas Propagat.*, vol. 61, no. 4, pp. 1704-1713, Apr. 2013.
- [6] P.G. de Gennes and J. Prost, *The Physics of Liquid Crystals*. 2nd ed. Clarendon Press, 1995.